

Superconducting States of Pure and Doped Graphene

Bruno Uchoa, and A. H. Castro Neto

Physics Department, Boston University, 590 Commonwealth Ave., Boston, MA 02215

We study the superconducting phases of the two-dimensional honeycomb lattice of graphene. We find two spin singlet pairing states, s -wave and an exotic $p + ip$ that is possible because of the special structure of the honeycomb lattice. At half filling, the $p + ip$ phase is gapless and superconductivity is a hidden order. We discuss the possibility of a superconducting state in metal coated graphene.

PACS numbers: 81.05.Uw, 74.78.-w, 74.25.Dw

Graphene is a two-dimensional (2D) electronic system on a honeycomb lattice whose electronic excitations can be described in terms of linearly dispersing Dirac fermions [1]. Because of its unusual properties [2], such as anomalous integer quantum Hall effect [3, 4] and universal conductivity [3], graphene has attracted a lot of attention in the condensed matter community. One of the interesting properties of graphene is that its chemical potential can be tuned through a electric field effect, and hence it is possible to change the type of carriers (electrons or holes), opening the doors for a carbon based electronics. Superconductivity has been induced in short graphene samples through proximity effect with superconducting contacts [5]. This indicates that Cooper pairs can propagate coherently in graphene. From the theoretical side, anomalous Andreev reflection [6] and transport [7] have been predicted in graphene junctions with superconductors. It is known that the electronic properties of graphene are modified by changing the number of graphene planes [8]. In particular, bilayer graphene has been demonstrated to be a tunable gap semiconductor [9]. These results raise the question of whether it would be possible to modify graphene, either structurally or chemically, so that it would become a magnet [10] or even an intrinsic superconductor. By exploring the number of graphene layers and the chemical composition, it maybe possible to tailor its electronic properties.

In this letter, we derive a mean-field phase diagram for spin singlet superconductivity in graphene. We show that besides the usual s -wave pairing, an unexpected spin singlet state with $p + ip$ orbital symmetry is possible because of the structure of the honeycomb lattice. In fact, we show that the $p + ip$ state is preferred to the s -wave state if the on-site electron-electron interactions are repulsive. $p + ip$ -pairing states are rather interesting [11] because, in the presence of a magnetic field, the superconducting vortices are described in terms of Majorana fermions with non-abelian statistics that can be used for topological quantum computing [12]. Although it is very hard to predict pairing mechanisms from microscopic models, we examine possible phonon and plasmon mediated superconductivity in chemically modified, metal coated, graphene, as shown in Fig. 1. Our results indicate that a plasmon mediated superconductivity is

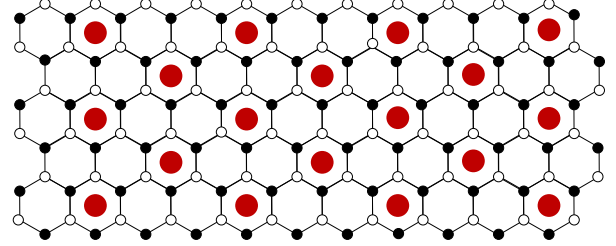


Figure 1: (color online) Graphene coated with metal. Small black (white) circles belong to the A (B) sublattices; Large (red) circles represent the metal atoms.

possible in this system.

Notice that on symmetry grounds an electronic state on a honeycomb lattice has three different components associated with the continuous $SU(2)$ spin symmetry and the discrete lattice symmetry (the honeycomb lattice can be described as a triangular lattice with a basis with two atoms, A and B, as in Fig. 1). At low energies and long wavelengths, close to the Dirac point, the system has effective $SO(3) \otimes Z_2$ spatial symmetry. Hence, the superconducting state can have a Cooper pair wavefunction of the form $\Psi_{\text{pair}} = \psi_S \otimes \psi_L \otimes \psi_{A-B}$, where ψ_S is the spin, ψ_L is the orbital, and ψ_{A-B} is the sub-lattice component. Pauli's principle requires the wavefunction to be anti-symmetric for the exchange of particles. For a spin singlet state, $S = 0$, one can have either $L = \text{even}$ and $A - B$ symmetric ($L = 0$ being the s -wave), or $L = \text{odd}$ and $A - B$ anti-symmetric ($L = 1$ being p -wave).

The free electron Hamiltonian can be written as:

$$H_t = -\mu \sum_i \hat{n}_{g,i} - t \sum_{\langle ij \rangle} \sum_{s=\uparrow\downarrow} (a_{i,s}^\dagger b_{j,s} + h.c.), \quad (1)$$

where $t \approx 2.8$ eV is the hopping energy between nearest neighbor C atoms, $a_{i,s}$ ($a_{i,s}^\dagger$) is the on-site annihilation (creation) operator for electrons in the sublattice A with spin $s = \uparrow, \downarrow$, and $b_{i,s}$ ($b_{i,s}^\dagger$) for sublattice B, $\hat{n}_{g,i}$ is the on-site particle density operator, and μ is the graphene chemical potential (we use units such that $\hbar = 1 = k_B$). Diagonalization of (1) leads to a spectrum given by: $\varepsilon_{\mathbf{k}} = -t|\gamma_{\mathbf{k}}|$, where \mathbf{k} is the 2D momentum, and $\gamma_{\mathbf{k}} = \sum_{\vec{\delta}} e^{i\mathbf{k}\cdot\vec{\delta}}$ ($\vec{\delta}_1 = a(\hat{x}/2 + \sqrt{3}/2\hat{y})$, $\vec{\delta}_2 = a(\hat{x}/2 - \sqrt{3}/2\hat{y})$, and $\vec{\delta}_3 = -a\hat{x}$, where $a \approx 1.42$ Å is the C-C distance).

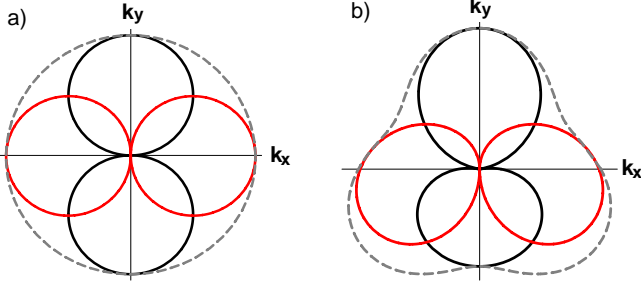


Figure 2: (color online) $p + ip$ order parameter in momentum space: (a) close to the Dirac point and (b) away from it. Dark (black) line is the real part, gray (red) is the imaginary part, and dashed is the amplitude of the order parameter.

At the corners of the hexagonal Brillouin zone (at $\mathbf{Q}_0 = [0, \pm 4\pi/(3\sqrt{3}a)]$), the band has the shape of a Dirac cone: $\varepsilon_{\mathbf{Q}_0+\mathbf{k}} = \pm v_0|\mathbf{k}|$, where $v_0 = 3at/2 \approx 6 \text{ eV \AA}$ is the Fermi-Dirac velocity. In neutral graphene, the chemical potential crosses exactly through the Dirac point ($\mu = 0$).

The electron-electron interactions are described by:

$$H_P = \frac{g_0}{2} \sum_{is} \left[a_{is}^\dagger a_{is} a_{i-s}^\dagger a_{i-s} + b_{is}^\dagger b_{is} b_{i-s}^\dagger b_{i-s} \right] + g_1 \sum_{\langle ij \rangle} \sum_{s,s'} a_{is}^\dagger a_{is} b_{js'}^\dagger b_{js'}, \quad (2)$$

where g_0 and g_1 are on-site and nearest neighbor electron-electron interaction energies, respectively. It is easy to see that the superconducting order parameters for spin singlet are: (1) s -wave: $\Delta_0 = \langle a_{i\downarrow} a_{i\uparrow} \rangle = \langle b_{i\downarrow} b_{i\uparrow} \rangle$; (2) p -wave: $\Delta_{1,ij} = \langle a_{i\downarrow} b_{j\uparrow} - a_{i\uparrow} b_{j\downarrow} \rangle$. We assume $\Delta_{1,ij} = \Delta_1$ for all nearest neighbors and zero, otherwise. In the momentum space one has: $\Delta_{\mathbf{k}} = \sum_{ij} \Delta_{1,ij} e^{-i\mathbf{k}\cdot(\mathbf{r}_i - \mathbf{r}_j)} = \Delta_1 \gamma_{\mathbf{k}}^*$. Close to the Dirac points \mathbf{Q}_0 (Fig. 2(a)) the order parameter can be written as, $\Delta_{\mathbf{Q}_0+\mathbf{k}} = (3a/2)\Delta_1(k_y + ik_x)$, that is, it has $p + ip$ symmetry. At high energies, away from the Dirac point, the discrete symmetry of the lattice is recovered and the pairing state is modified as in Fig. 2 (b). For simplicity, however, we refer to this phase as $p + ip$, which is the symmetry close the Dirac cone.

Decoupling the interaction terms in (2) gives,

$$H_P = E_0 + g_0 \Delta_0 \sum_i \left(a_{i\uparrow}^\dagger a_{i\downarrow}^\dagger + b_{i\uparrow}^\dagger b_{i\downarrow}^\dagger \right) + \text{h.c.} + g_1 \sum_{\langle ij \rangle} \Delta_{1,ij} \left(a_{i\uparrow}^\dagger b_{j\downarrow}^\dagger - a_{i\downarrow}^\dagger b_{j\uparrow}^\dagger \right) + \text{h.c.}, \quad (3)$$

and the total Hamiltonian can be diagonalized via a Bogoliubov transformation: $H_{\text{eff}} = \sum_{\mathbf{k}, \alpha, s} \omega_{\mathbf{k}\alpha s} \hat{n}_{\mathbf{k}\alpha s}^B + E_0$, where $E_0 = -g_0 \Delta_0^2 - 3g_1 \Delta_1^2$ (Δ_0 and Δ_1 are real numbers), and $\hat{n}_{\mathbf{k}, \alpha}^B$ is the quasi-particle number operator. The spectrum is: $\omega_{\mathbf{k}, \alpha, s} \equiv \alpha \omega_{\mathbf{k}, s}$, with $\alpha, s = \pm 1$ and,

$$\omega_{\mathbf{k}, s} = \sqrt{(t|\gamma_{\mathbf{k}}| + s\mu)^2 + (g_0 \Delta_0 + s g_1 \Delta_1 |\gamma_{\mathbf{k}}|)^2}. \quad (4)$$

For $\Delta_0 \neq 0$ and $\Delta_1 = 0$, eq. (4) describes an s -wave state with a gap given by: $E_g^{\{0\}} = 2|g_0 \Delta_0|$. In the case,

$\Delta_0 = 0$ and $\Delta_1 \neq 0$, the system has an isotropic gap $E_g^{\{1\}} = 2|\mu g_1 \Delta_1| / \sqrt{t^2 + g_1^2 \Delta_1^2}$, which scales linearly with μ . In the neutral limit ($\mu = 0$) for $\Delta_0 = 0$, the dispersion (4) is gapless, with $\omega_{\mathbf{k}, s} = \bar{t}|\gamma_{\mathbf{k}}|$, where \bar{t} is the effective hopping energy $\bar{t} = t\sqrt{1 + g_1^2 \Delta_1^2 / t^2}$, which renormalizes the Fermi-Dirac velocity. Notice that in this case, the superconducting state does not lead to a gap in the spectrum but to a renormalization of the velocity. This state of affairs we call hidden order. In the case for $\Delta_0 \neq 0$ and $\Delta_1 \neq 0$, particle-hole symmetry is broken and the gap is given by $E_g^{\{0,1\}} = 2|t g_0 \Delta_0 - g_1 \mu \Delta_1| / \bar{t}$.

The values of Δ_0 and Δ_1 are calculated by minimizing the free energy: $F = -\frac{1}{\beta} \sum_{\mathbf{k}, \alpha, s} \ln(1 + e^{-\beta \omega_{\mathbf{k}\alpha s}}) + E_0$, where $\beta = 1/T$. The coupled self-consistent equations for the order parameters are:

$$\Delta_0 = - \sum_{\mathbf{k}, s} (g_0 \Delta_0 + s |\gamma_{\mathbf{k}}| g_1 \Delta_1) \tanh(\beta \omega_{\mathbf{k}s} / 2) / (2\omega_{\mathbf{k}s}),$$

$$\Delta_1 = - \sum_{\mathbf{k}, s} |\gamma_{\mathbf{k}}| (g_1 \Delta_1 |\gamma_{\mathbf{k}}| + s g_0 \Delta_0) \tanh(\beta \omega_{\mathbf{k}s} / 2) / (6\omega_{\mathbf{k}s}).$$

For $\mu \neq 0$, one finds three distinct phases (see Fig. 3 (a)): (i) a s -wave phase for attractive on-site ($g_0 < 0$) and repulsive nearest neighbor ($g_1 > 0$) interactions; (ii) a $p + ip$ phase for repulsive on-site ($g_0 > 0$) and attractive nearest neighbor interactions ($g_1 < 0$); and (iii) a co-existence phase for fully attractive interactions ($g_0, g_1 < 0$). The superconducting transitions from normal to s -wave, and normal to $p + ip$ are of second order. The transitions involving the mixed phase for $g_0 < 0$ and $g_1 \rightarrow 0$ or $g_1 < 0$ and $g_0 \rightarrow 0$ are of first-order even at $T = 0$. At the critical temperature, T_c , the phase transitions of phases (i) and (ii) to the normal state are second order, while the transition between the mixed phase and the normal phase is abrupt. In the weak coupling limit of phase (i), i.e. for $|g_0| \ll -g_0^c \equiv \pi v_0^2 / \Lambda$, where Λ is a high energy cut-off, the critical temperature is given by [13]: $T_c \approx 2\mu(\gamma/\pi) \exp\{-\Lambda(g_0^c/g_0 - 1)\mu^{-1} - 1\}$, where $\ln \gamma \sim 0.577$ is the Euler constant. In reality, however, because the system is 2D there can be no true superconducting long-range order (Mermin-Wagner theorem) but there will be a Kosterlitz-Thouless (KT) transition below a certain temperature $T_{KT} < T_c$. Hence, T_c only establishes the temperature below which the amplitude of the order parameter becomes finite while its phase still fluctuates. Phase coherence only occurs at low temperatures and depends on the phase stiffness of the system. Although the transition is of the KT type, one expects a precipitous drop of the resistivity of the material below T_{KT} indicating the entrance of the electrons into a state of quasi-long-range superconducting order.

For $\mu = 0$ superconductivity requires a minimum coupling to occur (the problem becomes quantum critical). The quantum critical lines are given by $g_0 = g_0^c \equiv -\pi v_0^2 / \Lambda$ and $g_1 = g_1^c \equiv -4\pi v_0^4 / (a^2 \Lambda^3)$, as shown in Fig. 3 (b). We identify the phases: (iv) s -wave for $g_0 < g_0^c$

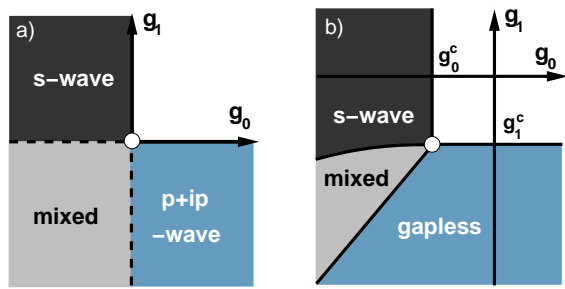


Figure 3: Mean-field phase diagram: (a) $\mu \neq 0$; (b) and $\mu = 0$. Dashed lines are first order transitions, continuous lines are second order.

and $g_1 > f(g_0) \equiv g_0^2 g_1^c / [g_0^2 - (3/2)(g_0 - g_0^c)^2]$; (v) gapless phase, for $g_1 < h(g_0) \equiv 4[v_F^2 / (a^2 \Lambda^2)] g_0 < g_1^c$; and (vi) mixed phase, for $h(g_0) < g_1 < f(g_0)$, where the symmetry is mixed between s and $p + ip$ pairing.

We remark that the physical realization of superconductivity in neutral graphene is difficult because of the vanishing density of states and the absence of electron-electron screening. Therefore, in order to superconductivity to develop easily one has to substantially shift the graphene chemical potential away from the Dirac point. This can be achieved by chemically doping graphene with a metal coating: when an alkaline metal is placed on top of a graphene crystal, the s electrons migrate to the π -band to compensate the strong difference in electronegativities, raising up the chemical potential from the Dirac points and lowering the energy of the metallic bands in order to establish electrostatic equilibrium. Since neither carbon nor alkaline metals alone superconduct in ordinary conditions, we identify two main possible mechanisms for superconductivity on coated graphene: 1) *electron-phonon* coupling of the ions with the electrons in the modified metallic bands, and 2) *electron-plasmon* coupling of the graphene electrons with the acoustic plasmons of the metal.

The electron-phonon mechanism tends to favor superconductivity at *high* electronic densities, and has been used to explain the bulk superconductivity of graphite intercalated CaC_6 [14, 15, 16]. The strength of the electron-phonon coupling can be extracted from *ab initio* calculations and from experimental data, which are not currently available for coated graphene. Nevertheless, this mechanism is conventional and we will not discuss it here.

In the electron-plasmon mechanism, the attractive electron-electron interaction is mediated by a screened acoustic plasmon of the metal, which is favorable to superconductivity at *low* electronic densities, where the plasmon is weakly damped by the graphene particle-hole continuum. In the remaining of the letter we investigate under what conditions this mechanism could be effective for graphene superconductivity. Since electrons and

acoustic plasmons have comparable energy scales, a reliable calculation of the critical temperature requires the study of retardation effects that we will cover in future publications.

Plasmon mediated superconductivity has been widely studied in the past [17, 18, 19, 20, 21] and we concentrate on the particular aspects of the graphene problem. In coated graphene, the Coulomb interaction between the layers induces an effective electron-electron interaction for electrons in the graphene layer that can be calculated with the use of the random phase approximation (RPA) [22]. The RPA expansion in terms of the zeroth order polarization functions of the metal, Π_m^0 , and of graphene, Π_g^0 , results in an effective *retarded* interaction of the form:

$$H_{ef}^g = \sum_{\mathbf{q}} \sum_{\omega} V_{ef}(\mathbf{q}, \omega) \hat{n}_g(\mathbf{q}, \omega) \hat{n}_g(-\mathbf{q}, -\omega), \quad (5)$$

where,

$$V_{ef}(\mathbf{q}, \omega) = V_{0,q} / \epsilon(\mathbf{q}, \omega) [1 - (V_{0,q} - V_{d,q}) \Pi_m^0(\mathbf{q}, \omega)], \quad (6)$$

is the effective electron-electron interaction, and

$$\begin{aligned} \epsilon(\mathbf{k}, \omega) = & 1 - V_{0,q} [\Pi_g^0(\mathbf{k}, \omega) + \Pi_m^0(\mathbf{k}, \omega)] \\ & + (V_{0,q}^2 - V_{d,q}^2) \Pi_m^0(\mathbf{k}, \omega) \Pi_g^0(\mathbf{k}, \omega) \end{aligned} \quad (7)$$

is the total dielectric function of the system, with $V_{d,q} = 2\pi e^2 e^{-qd} / (\epsilon_0 q)$ as the Fourier transform of the Coulomb interaction between electrons in two layers separated by a distance d . In Eq. (7), the separation between the metal and graphene layers induces a cross polarization term between the two layers that vanishes when $d = 0$. In the opposite limit, $kd \gg 1$, the two layers decouple.

The electronic susceptibility of metals is commonly described by the Lindhard polarization function. When $\omega > v_F q$, where v_F is the Fermi velocity of the metal, the $q \rightarrow 0$ limit of the 2D Lindhard function gives [22] $V_{0,q} \Pi_m^0(q, \omega) = \Omega_m^2 / \omega^2$, where $\Omega_m(q) = e \sqrt{2E_F q} / \epsilon_0$ is the plasmon of the 2D electron gas, and E_F is the Fermi energy of the metallic band. The polarization function of graphene at small momentum q is dominated by intra-band excitations connecting states in the same branch of the Dirac cone. At lowest order, it has the same momentum and frequency dependence of the polarization function of an infinite stack of graphite layers in the absence of interplane hopping [23]:

$$\Pi_g^0(q, \omega) = -(2\mu / \pi v_0^2) \left[1 - \omega / \sqrt{\omega^2 - v_0^2 q^2} \right]. \quad (8)$$

In the low frequency limit, $\omega \ll v_0 q$, the polarization function of graphene is approximated by its static part, $\Pi_g^0(q, 0)$, and the total dielectric function (7) becomes $\epsilon(q, \omega) = \epsilon_g(q, 0) [1 - \Omega_p^2(q) / \omega^2]$, where,

$$\Omega_p^2(q) \approx \Omega_m^2(q) / \epsilon_g(q, 0) [1 - (1 - e^{-2qd}) V_{0,q} \Pi_g^0(q, 0)], \quad (9)$$

is the screened plasmon mode of the metal (i.e., $\epsilon(q, \Omega_p(q)) = 0$). When $qd \ll 1$ and $|\omega| \ll v_0q$, this plasmon has a linear dispersion, $\Omega_p(q) \approx \sqrt{E_F^*/(2\mu)}v_0q$, where $E_F^* = E_F [1 + (8e^2d\mu/\epsilon_0v_0^2)]$. For $qd \gg 1$, the plasmon is not screened by the graphene layer, and one recovers the plasmon dispersion for the 2D electron gas: $\Omega_p \rightarrow \Omega_m \propto \sqrt{q}$. In the region $v_Fq < |\omega| \ll v_0q$, eq. (6) can be approximated as:

$$V_{ef}(q, \omega) \approx V_{0,q}/\epsilon_g(q, 0) [\Omega_p^2/(\omega^2 - \Omega_p^2) + 1], \quad (10)$$

In the attractive region 1 of Fig. 4, the electrons of graphene screen the charge fluctuations, restoring the longitudinal response of the collective modes in the normal phase, that is required to preserve the local gauge invariance of the superconductor in the London limit [24]. The electrons of the metal by their turn are slow and tend to anti-screen the graphene electrons [25], producing an average repulsive interaction in the metallic band. In the high frequency limit $|\omega| \gg v_0q$, the effective interaction (6) has a second region of attraction (region 2 of Fig. 4). For $qd \ll 1$, the effective interaction in this region can be approximated by $V_{ef}(q, |\omega| \gg v_0q) \approx V_{0,q} [\Omega_{2D}^2/(\omega^2 - \Omega_{2D}^2) + 1]$, where $\Omega_{2D}(q) = e\sqrt{2(E_F + \mu)q}/\epsilon_0$ is the plasmon dispersion of the 2D electron gas. Although the interaction is attractive for $|\omega| < \Omega_{2D}(q)$, this attractive region is present in the ordinary 2D electron gas and it does not lead itself to superconductivity, although it favors superconductivity by reducing the Coulomb repulsion.

A necessary condition for appearance of plasmon induced superconductivity is that the screened acoustic plasmon is not overdamped by the particle-hole continuum in the interval $v_Fq < \Omega_p \lesssim v_0q$. In the long wave-

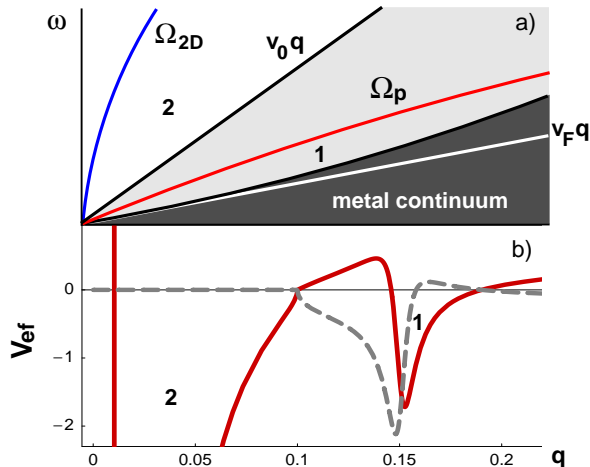


Figure 4: a) Low energy excitations in the metal-graphene system. Dark and grey regions are the particle-hole continuum of the metal and of graphene, respectively. b) Real (solid) and imaginary (dashed) parts of the effective interaction (6), in units of $2\pi e^2 v_0 / (\epsilon_0 \mu) \sim 45 \text{ eV \AA}^2$ vs. momentum normalized by μ/v_0 , for $\omega = 0.1\mu$, $\mu = 2 \text{ eV}$, $E_F = 0.4 \text{ eV}$.

length limit, $qd \ll 1$, the condition for the existence of this acoustic mode is $E_F \lesssim 2\mu\epsilon_0/(\epsilon_0 + 8\alpha_g d\mu/v_0) < mv_0^2/2 \approx 2.4 \text{ eV}$. For $\mu \sim 2 \text{ eV}$, $\epsilon_0 \sim 5$ and $d \sim 3 \text{ \AA}$ [26], the left hand side of the inequality becomes $E_F \lesssim 1 \text{ eV}$, or equivalently that the electronic concentration in the metal layer has to be smaller than $\sigma_c \approx 4 \times 10^{14} \text{ electrons cm}^{-2}$ (or 0.12 electrons per C). If x is the number of remaining electrons per metallic atom M, for a system with chemical composition $[M_n C_m]_{2D}$, one of the conditions is that $x \lesssim 0.12(m/n)$. For K coated graphene $[KC_8]_{2D}$, which is known to form a stable metallic lattice [27], the condition is $x \lesssim 0.96$ electrons per K. Values of $x \sim 0.54-0.83$ were obtained by *ab initio* calculations for K adsorbed in graphite [27].

In conclusion, we have derived the mean-field phase diagram for superconductivity in a honeycomb lattice, where a novel singlet $p+ip$ phase appears. We have examined the mechanism of plasmon mediated superconductivity in graphene with the aim of proposing new carbon low-dimensional systems where superconductivity can be observed.

We thank V. Falko, F. Guinea, N. M. R. Peres, and S.-W. Tsai for many discussions and comments. This work was supported by NSF grant DMR-0343790. B. U. acknowledges CNPq, Brazil, for the support under the grant 201007/2005-3.

-
- [1] K. S. Novoselov *et al.*, Science **306**, 666 (2004).
 - [2] N. M. R. Peres, *et al.*, Phys. Rev. B **73**, 125411 (2006).
 - [3] K. S. Novoselov *et al.*, Nature **438**, 197 (2005).
 - [4] Y. Zhang *et al.*, Nature **438**, 201 (2005).
 - [5] H. B. Heersche *et al.*, Nature **446**, 56 (2007).
 - [6] C.W.J. Beenakker, Phys. Rev. Lett. **97**, 067007 (2006).
 - [7] M. Titov *et al.*, Phys. Rev. B **75**, 045417 (2007)
 - [8] F. Guinea, *et al.*, Phys. Rev. B **73**, 245426 (2006).
 - [9] E. V. Castro *et al.*, cond-mat/0611342.
 - [10] N. M. R. Peres, *et al.*, Phys. Rev. B **72**, 174406 (2005).
 - [11] I. F. Foulkes, *et al.*, Phys. Rev. B **15**, 1395 (1977).
 - [12] D. A. Ivanov, Phys. Rev. Lett. **86**, 268 (2001).
 - [13] B. Uchoa *et al.*, Phys. Rev. B **71**, 184509 (2005).
 - [14] G. Lamura, *et al.* Phys. Rev. Lett. **96**, 107008 (2006).
 - [15] I. I. Mazin, Phys. Rev. Lett. **95**, 227001 (2005).
 - [16] M. Calandra *et al.*, Phys. Rev. Lett. **95**, 237002 (2005).
 - [17] H. J. Fröhlich, J. Phys. C **1**, 544 (1968).
 - [18] C. F. Richardson *et al.*, Phys. Rev. B **55**, 15130 (1997).
 - [19] A. Bill *et al.*, Phys. Rev. B **68**, 144519 (2003).
 - [20] J. Ruvalds, Phys. Rev. B **35**, 8869 (1987).
 - [21] V. Kresin *et al.*, Phys. Rev. B **13**, 7854 (1988).
 - [22] D. Pines, *Elementary excitations in solids* (Perseus, 1999).
 - [23] K. W. -K. Shung, Phys. Rev. B **34**, 979 (1986).
 - [24] D. Pines, J. R. Schrieffer, Nuovo Cimento **10**, 496 (1958).
 - [25] J. W. Garland, Phys. Rev. Lett. **11**, 111 (1963).
 - [26] D. B. Lamoen *et al.*, Jou. Chem. Phys. **108**, 3332 (1998).
 - [27] M. Caragiu, S. Finberg, J. Phys.: Condens. Matter **17**, R995 (2005), and references therein.